Kinetics and Catalysis, Vol. 41, No. 3, 2000, pp. 415–428. Translated from Kinetika i Kataliz, Vol. 41, No. 3, 2000, pp. 457–471.

Mechanisms of Reactions between >Si=O Groups and CO_2, N_2O, and HC≡CH Molecules: An Experimental and Quantum Chemical Study

V. A. Radtsig, I. V. Berestetskaya, and I. V. Kolbanev

Semenov Institute of Chemical Physics, Russian Academy of Sciences, Moscow, 117977 Russia

Received December 30, 1998

Abstract—IR spectroscopy and quantum chemical calculations are used to study the directions and kinetics of reactions between silanone groups $(\equiv Si–O)_2Si=O$ and CO_2, N_2O, and acetylene molecules. IR bands are assigned on the basis of the calculation of vibrational spectra of model low-molecular systems. Quantum chemical methods are used to obtain the data on the shapes of potential energy surfaces of these systems (intermolecular complexes and transition states). These data are used to interpret kinetic data. The silanone group is inclined to the formation of relatively stable (~10 kcal/mol) intramolecular complexes with CO_2, N_2O, and acetylene molecules. Their geometries and electronic structures are determined.

INTRODUCTION

The $R_2Si=O$ compounds containing a silanone group were first stabilized using the matrix-isolation technique [1–5]. The first experiments identified that, in contrast to the carbonyl group, the silanone group is characterized by a high reactivity. Specifically, it undergoes dimerization at very low temperatures. Because the isolation and stabilization of silanone groups is difficult, the experimental data on the mechanisms of relevant reactions and especially quantitative characteristics of the corresponding processes are rather limited.

The first experimental evidence for the fact that the $(\equiv Si–O)_2Si=O$ groups can be stabilized on the surface of mechanically activated silica were obtained in [6]. Then, the method was developed for their synthesis on the surface of reactive silica (RSi) [7, 8]. Silanone groups stabilized on the silica surface are thermally sta-

EXPERIMENTAL METHODS AND QUANTUM CHEMICAL CALCULATIONS

Experiments were carried out with samples of high-dispersed A-300 aerosil in the form of semitransparent films (50- to 100-μm thick). The procedure for RSi sample preparation was analogous to that developed earlier [10, 11].

IR spectra were registered on a Digilab Fourier-transform IR spectrometer (256–1024 scans and 4-cm^{-1} resolution). A sample was placed into a special section of the working chamber equipped with two silicon windows.

Quantum chemical calculations were carried out using molecular models of the groups on the solid surface. As shown in [12, 13], the experimentally observed properties of fragments with a silica-surface silicon atom bound to two or three lattice oxygen atoms ((≡Si–

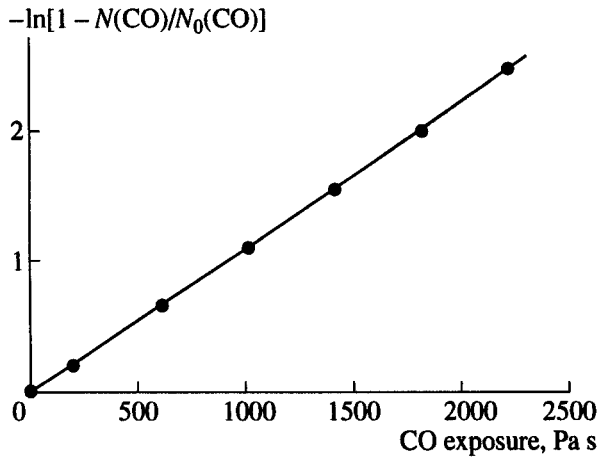

Fig. 1. Kinetics of CO chemisorption during the reaction $>Si<\overset{O}{\underset{O}{\diagup\diagdown}} + CO \longrightarrow >Si<\overset{O}{\underset{O}{\diagup\diagdown}}C{=}O$ at 298 K.

MP2/6-31G** level were corrected by a scale factor of 0.961 [18]. According to the results obtained, DFT gives better results for vibrational spectra simulation.

For empirical correction $\nu(1)_{corr}$ of the calculated value $\nu(1)_{corr}$ of the normal vibration frequency, we calculated the frequency of analogous vibrations in a structurally similar molecule $\nu(2)_{calc}$ and compared it to the available experimental frequency $\nu(2)_{exp}$. Then, the correction was introduced as follows:

$$\nu(1)_{corr} = \nu(1)_{calc}\{\nu(2)_{exp}/\nu(2)_{calc}\}. \quad (1)$$

This value was correlated to the experimental data.

RESULTS AND DISCUSSION

1. Kinetic and Thermochemical Characteristics of Silanone and Carbonate Group Synthesis

According to [7, 8], diamagnetic defects on the RSi sample surfaces are mostly silylene groups $(\equiv Si{-}O)_2Si{:}$. Their concentration is ~10^{13} group/cm^2. To obtain silanone groups from them, we used procedures developed in [6–8, 11]. Silylene groups were first oxidized by molecular oxygen to form dioxasiliranes [7, 8, 11]:

$$(\equiv Si{-}O)_2Si{:} + O_2 \longrightarrow (\equiv Si{-}O)_2Si<\overset{O}{\underset{O}{}} \quad (I)$$

This reaction occurs at room temperature. Its rate constant is $1.3 \times 10^{-13}\exp(-8/RT)$ cm^3 molecule^{-1} s^{-1}, and the activation energy is given in kcal/mol [7, 8]. The reaction heat is ~75 kcal/mol.

Dioxasilirane groups were then converted into the carbonate form using CO molecules:

$$(\equiv Si{-}O)_2Si<\overset{O}{\underset{O}{}} + CO \xrightarrow{300\ K} (\equiv Si{-}O)_2Si<\overset{O}{\underset{O}{\diagup\diagdown}}C{=}O \quad (II)$$

This reaction is highly exothermic by ~95 kcal/mol [19]. CO consumption follows the rate law $dN(CO)=dN(>Si<O_2)$ at 298 K (Fig. 1):

$$-dN(CO)/dt = KP(CO)N\left(>Si<\overset{O}{\underset{O}{}}\right)$$

The CO pressure over a sample decreased during the reaction. Therefore, instead of time-axis, we plotted the data against CO exposition $\left(\int P(CO)dt\right)$, which is proportional to the number of molecular collisions with surface sites [20]. $N_0(CO)$ and $N(CO)$ are the total and current numbers of chemisorbed CO molecules. The rate constant determined from the slope of this line is $k = (4.2 \pm 0.3) \times 10^{-18}$ cm^3 molecule^{-1} s^{-1}.

The activation energy is 7.3 kcal/mol assuming a preexponential factor of 10^{-12} cm^3 molecule^{-1} s^{-1}. A change in the value of the preexponential factor from 10^{-11} to -10^{-13} cm^3 molecule^{-1} s^{-1} leads to a change of the activation energy from 8.7 to 6.0 kcal/mol.

Silanone groups were obtained by the thermal decomposition of carbonates [6, 9]:

$$(\equiv Si{-}O)_2Si<\overset{O}{\underset{O}{\diagup\diagdown}}C{=}O \xrightarrow{500\ K} (\equiv Si{-}O)_2Si{=}O + CO_2. \quad (III)$$

The reaction heat is 37 ± 1 kcal/mol according to calorimetric measurements [6, 21].

The reverse reaction

$$(\equiv Si{-}O)_2Si{=}O + CO_2 \longrightarrow (\equiv Si{-}O)_2Si<\overset{O}{\underset{O}{\diagup\diagdown}}C{=}O \quad (IV)$$

of carbonate formation occurs even at room temperature. We only managed to estimate the activation energy of this reaction: $E_{app} = (2 \pm 2)$ kcal/mol. When studying the bimolecular reactions of silanone groups and gaseous molecules, the pressure in a working chamber usually was ~10^{-2} torr. Under these conditions, we were able to measure the reaction rates with $k(298\ K) < 3 \times 10^{-17}$ cm^3 molecule^{-1} s^{-1}. Faster reactions were controlled by diffusion of gaseous molecules from the volume of the system to the sample. Bimolecular reactions of silanone groups with CO_2, N_2O and HC≡CH molecules studied in this work were controlled by diffusion. Assuming a preexponential factor of 10^{-12} cm^3 molecule^{-1} s^{-1}, the activation energies of these reactions were lower than 4.5 kcal/mol. In other words, $E_{app} = (2 \pm 2)$ kcal/mol.

Based on the experimental data, we may estimate the activation energy of reaction (III) as 39 ± 3 kcal/mol. This value combines the enthalpy of this reaction and the activation energy of reverse reaction (IV).

2. Structure and Vibrational Spectrum of Carbonate

$$(\equiv Si\text{–}O)_2Si\langle^{O}_{O}\rangle C{=}O$$

A carbonate complex on the silica surface has intense bands in the IR spectrum at 1931 and 891 cm^{-1} [9, 10]. They have similar extinction coefficients, and the corresponding transitions are characterized by similar oscillator strengths [9]. Heating the carbonate-containing samples at 550 K was accompanied by their decomposition (reaction (III)) and silanone group regeneration. Silanone groups had an IR band at 1306 cm^{-1} [9].

When preparing carbonates (reactions (I) and (II)), we also used isotope-labeled molecules $^{18}O_2$ with admixed $^{16}O^{18}O$ (~30%) and/or $^{13}C^{16}O$ with admixed $^{12}C^{16}O$ (~13%). This enabled us to obtain the experimental data on the values of isotopic shifts of the bands in IR spectra of the carbonate. Figure 2 and Tables 1 and 2 summarize the results obtained.

Morterra and Low [10] assigned the band at 1931 cm^{-1} to the stretching vibrations of the C=O group in the carbonate-like structure, although these authors assumed a different structure for chemisorption sites on the RSi surface. Therefore, Morterra and Low assigned this band to the carbonate with the structure ≡Si–O–(C=O)–O–Si≡ and were surprised with such a high value of the C=O stretching frequency. (A usual value is by almost 60 cm^{-1} lower.) The cyclic structure of the carbonate was proposed in [6, 8].

To interpret the experimental data, we used the simulated vibrational spectra for the molecules (including isotopically substituted molecules), containing a carbonate fragment. Figure 3 and Tables 3–5 specify the optimized geometries, energies, and normal vibration frequencies for the following molecules: $F_2Si\langle^{O}_{O}\rangle C{=}O$ **(III)**, $(H_3Si\text{–}O)_2Si\langle^{O}_{O}\rangle C{=}O$ **(IV)**, $(F_3Si\text{–}O)_2Si\langle^{O}_{O}\rangle C{=}O$ **(V)**. For empirical correction (1) of C=O vibration frequencies, we used $F_2C{=}O$ as a reference molecule (no. 5, Tables 3, 5) for which the experimental frequency of the stretching C=O vibration is 1928 cm^{-1} [22]. In this molecule (as in the carbonate structure), carbon binds to the electronegative substituents (fluorine atoms). According to calculation, the lengths (Table 3) and frequencies (Tables 5, in boldface) of stretching vibrations of C=O in these molecules are close.

The frequency of C=O vibration depends on substituents (F, H_3Si–O, or F_3Si–O) at a surface silicon atom and decreases by ~30 cm^{-1} as electronegativity decreases within the series F, F_3Si–O, H_3Si–O. For the molecules containing electronegative substituents (F and F_3Si–O), which are close to the surface defects in silica, the calculated frequency compares well to the value obtained for the carbonate on SiO_2.

The results of calculations were used to assign experimental frequencies of C=O stretching for isotope-containing carbonate structures (Fig. 2a and Table 1). Note that an experimental decrease in the frequency of $^{12}C{=}^{16}O$ stretching (~3 cm^{-1}) during the isotopic substitution of oxygen atoms in the cycle is not reflected in calculations.

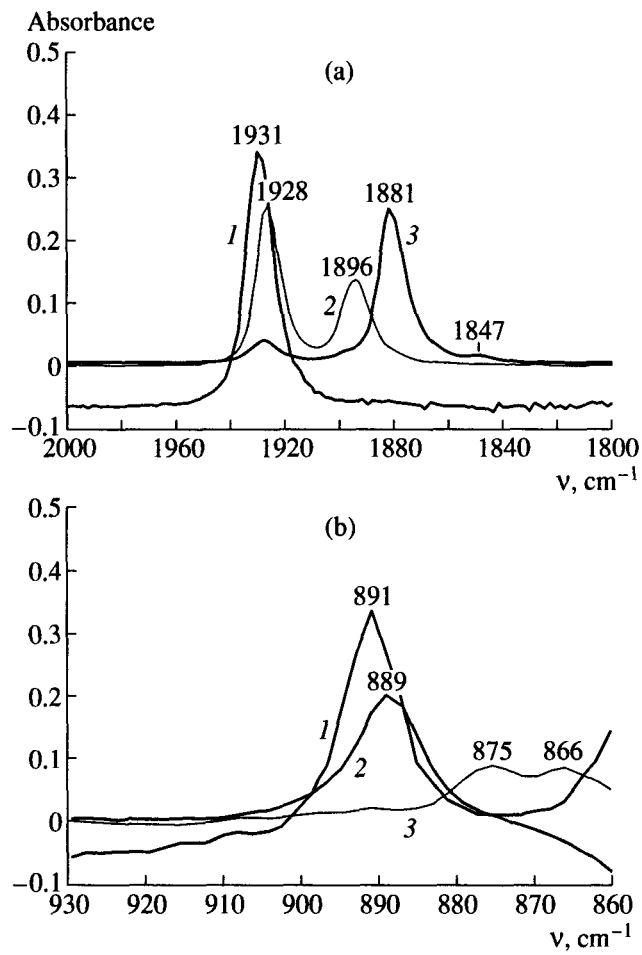

Fig. 2. IR spectra of carbonates $>Si\langle^{O}_{O}\rangle C{=}O$ with different isotopic compositions. CO and O_2 molecules of the following isotopic compositions were used in the synthesis of carbonates by reactions (I) and (II): (*1*) $^{16}O_2$, $^{12}C^{16}O$; (*2*) $^{18}O_2$ and $^{12}C^{16}O$; (*3*) $^{16}O_2$ and $^{13}C^{16}O$.

The above results support the assumed structure of the surface carbonate [6, 8]. Internal strain in the four-membered ring results in weakening of C–O bonds and, as a consequence, in strengthening of C=O bonds together with a higher frequency of its vibration.

For the normal vibration with a frequency of 891 cm^{-1}, the following characteristic features were found: (1) high band intensity, (2) involvement of oxygen atoms from the four-membered ring in this vibration (the highest isotopic shift of the band was registered when $^{18}O_2$ (reaction (I)) was used), (3) a small shift of the band when ^{12}C was replaced by ^{13}C (Fig. 2b and Table 2).

Table 1. Frequencies of stretching vibrations of C=O bonds in the >Si<O_2>C=O groups of different compositions (cm^{-1})

Isotopic composition	ν, cm^{-1}		
	experiment	calculation*	
>Si<$^{16}O_2$>^{12}C=^{16}O	1931 ± 1	1931	1931
>Si<$^{18}O_2$>^{12}C=^{16}O** +	1928 ± 1	1931	1931
>Si<$^{16}O^{18}O$>^{12}C=^{16}O		1931	1931
>Si<$^{16}O_2$>^{12}C=^{18}O** +	1896 ± 1	1894	1894
>Si<$^{16}O^{18}O$>^{12}C=^{18}O		1894	1894
>Si<$^{16}O_2$>^{13}C=^{16}O	1881 ± 1	1882	1882
>Si<$^{16}O_2$>^{13}C=^{18}O** +	1847 ± 1	1843.5	–
>Si<$^{16}O^{18}O$>^{13}C=^{18}O		1843.5	–

* The first and second columns refer to the DFT calculation of the $F_2Si<O_2>C=O$ and $F_6O_2Si_3<O_2>C=O$ molecules. Frequencies are scaled so that the calculated and experimental frequencies coincided for the >Si<$^{16}O_2$>^{12}C=^{16}O fragment.

** Experimental spectrum may be a superposition of signals from the structures of the indicated isotopic composition.

Table 2. Isotopic shifts of the IR band at 891 cm^{-1} in carbonate spectra

Isotopic composition	ν, cm^{-1}		
	experiment	calculation*	
>Si<$^{16}O_2$>^{12}C=^{16}O	891 ± 1	891	891
>Si<$^{16}O_2$>^{13}C=^{16}O	889 ± 1	889	889
>Si<$^{16}O^{18}O$>^{12}C=^{16}O** +	875 ± 1	872	876
>Si<$^{16}O^{18}O$>^{12}C=^{18}O		869	–
>Si<$^{18}O_2$>^{12}C=^{16}O	866 ± 1	854	861

* For notes see Table 1.

According to the calculation, several normal vibrations of dicarbonate molecules **III–V** should be observed at 800–1000 cm^{-1} for the atoms involved in the ring. In Fig. 3, arrows point to the directions of atomic shifts for a normal vibration corresponding to the above conditions. The frequencies of this vibration in different carbonate molecules **III–V** with different substituents at a silicon atom are close (901–908 cm^{-1}; in boldface in Table 5). Table 2 shows the isotopic shifts of this normal vibration. The calculated values agree well with the experiment.

A similar isotopic shift ($^{16}O \longleftrightarrow {}^{18}O$) was experimentally observed for the $(R_2SiO)_2$ molecules (R is mesityl) in which a four-membered ring contains two silicon atoms [23]. The isotopic substitution resulted in a shift of a band assigned to the ring vibrations from 828 cm^{-1} to 802 cm^{-1}. Thus, despite some difference in the chemical structure of these four-membered rings, similar normal vibrations of ring atoms have similar isotopic shifts.

The cyclic structure $(\equiv Si–O)_2Si<\begin{matrix}O\\O\end{matrix}>Si(O–Si\equiv)_2$, containing two silicon atoms, can be formed on the silica surface in the process of its dehydration [23, 24]. The IR bands at 908 and 888 cm^{-1} were assigned to the vibrations of oxygen atoms in the four-membered ring. They have comparable intensities and fall in the same spectral range as those of carbonate. Note that, in the case of $(\equiv Si–O)_2Si<\begin{matrix}O\\O\end{matrix}>Si(O–Si\equiv)_2$ groups, the symmetric arrangement of atoms in the cycle, which is characteristic of the $>Si<\begin{matrix}O\\O\end{matrix}>C=O$ fragment, can brake. Indeed, the geometric structure of the fragment is controlled by the spatial configuration of four silicon atoms that comprise the next coordination sphere of a defect. This configuration should not be symmetric. In this case, the ring would be deformed and this deformation may be reflected in the IR spectrum.

3. Mechanism of CO_2 Addition to a Silanone Group

We calculated the profiles of the potential energy surface for the $CO_2 + F_2Si=O$ system, which served as a model for the reaction between the surface silanone group and CO_2 molecule. Figure 4 shows the energetic diagram of the process.

When molecules approach each other, a molecular complex **I** is formed (see Fig. 3 and Tables 3–5) in which one of the oxygen atoms of a CO_2 molecule approaches a silicon atom. The formation heat of this complex is rather high (~10 kcal/mol). Neither for this system nor for two other systems (*vide infra*), did we analyze the nature of the transition state for the formation of the intramolecular complex from separate molecules. We may assume that the activation barrier for the formation of the intramolecular complex should be low. According to experimental estimates (*vide infra*), its height is 2 ± 2 kcal/mol.

The deepest minimum on the potential energy surface corresponds to the formation of the carbonate structure **III**. Comparison of the experimental data and the data for the surface silanone groups with a CO_2 molecule shows that calculations underestimated the value for the reaction heat by 5–10 kcal/mol. For the calculations at the DFT and MP2/6-31G** levels, this situation is quite typical.

Figure 3 and Tables 3–5 show the structure and characteristics of the transition state **II**, which separates two stable states of the system—the intermolecular complex and carbonate. Figure 3 shows the directions of atomic shifts as the systems moves along the reaction coordinate. The value of the activation energy of intramolecular complex transition into carbonate is only 2.3 (1.6) kcal/mol. The transition state has a lower energy than free CO_2 and $F_2Si=O$ molecules.

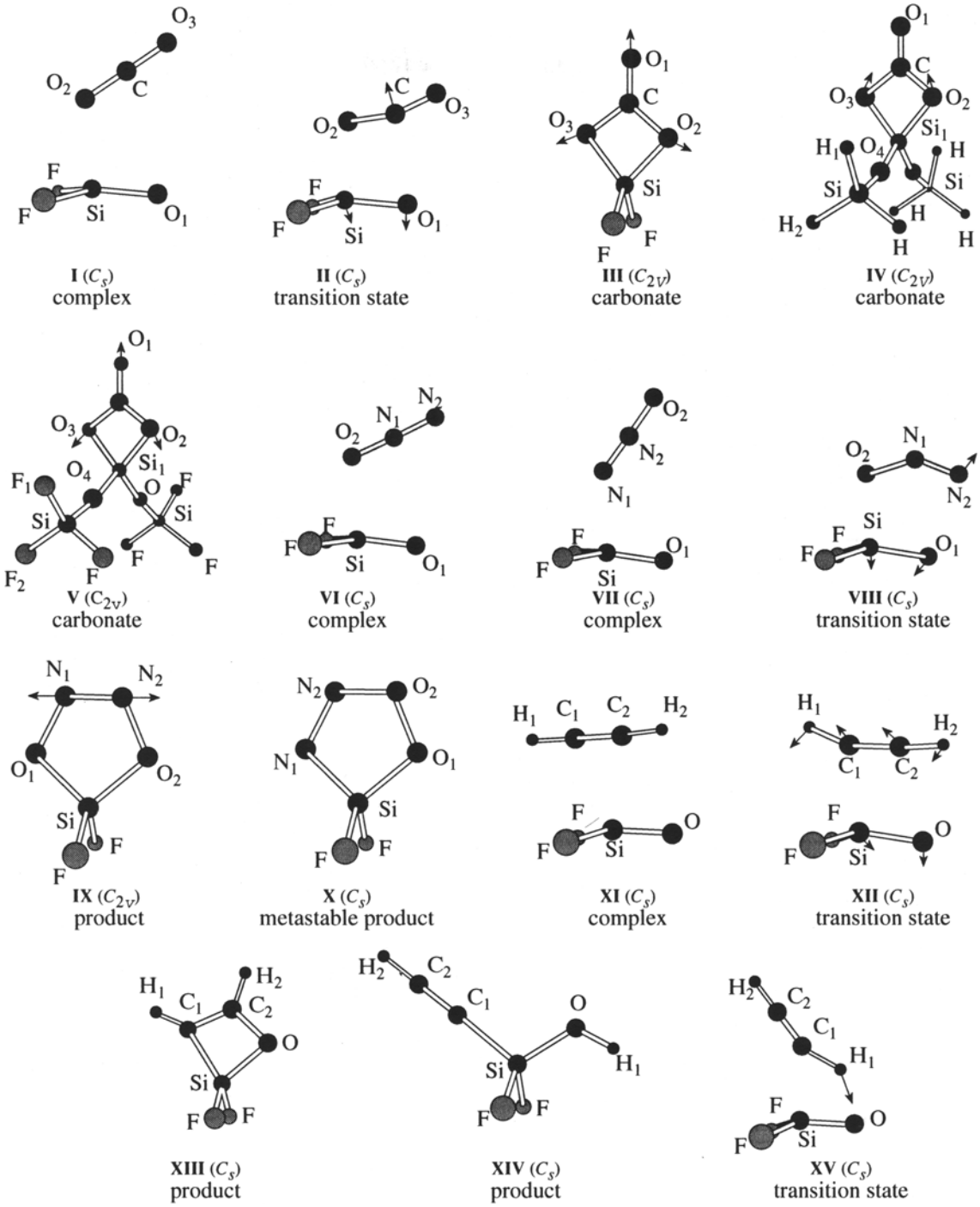

Fig. 3. Spatial configurations, symmetry, and atom numbering in molecules and radicals.

Taking into account that silanone forms a rather stable intermolecular complex with a CO_2 molecule, the kinetic scheme for carbonate formation can be described as follows:

$$(\equiv Si{-}O)_2Si{=}O + CO_2 \underset{k_{-1}}{\overset{k_1}{\rightleftarrows}} (\text{complex}) \xrightarrow{k_2} (\equiv Si{-}O)_2Si\langle{}^{O}_{O}\rangle C{=}O$$

Using the theory of steady-state concentration, the apparent rate constant of the reaction is $k_{app} = k_1k_2/(k_{-1} + k_2)$. Depending on the ratios of k_{-1} and k_2, two extreme situations are possible. According to the calculation, the value of the activation barrier for complex decomposition is higher than that of carbonate formation. This allows us to assume that for this reaction $k_2 \gg k_{-1}$, $k_{app} \cong k_1$, and the reaction rate is equal to the formation

Table 3. Optimized geometries*

No.	Structure	Parameters
1	$F_2Si{=}O$ (C_{2v})	$R(SiO) = 1.510$, $R(SiF) = 1.586$, $\angle OSiF = 127.9$
2	$O{=}C{=}O$	$R(CO) = 1.118$
3	$N{=}N{=}O$	$R(NN) = 1.126$, $R(NO) = 1.184$
4	$H{-}C{\equiv}C{-}H$	$R(CC) = 1.443$, $R(CH) = 1.085$
5	$F_2C{=}O$ (C_{2v})	$R(CO) = 1.171$, $R(CF) = 1.321$, $\angle OCF = 126.2$
6	F_2SiO_3C (C_s, **I**)	$R(SiO_1) = 1.516$, $R(SiF) = 1.592$, $R(SiO_2) = 2.171$, $R(O_2C) = 1.178$, $R(CO_3) = 3.018$, $\angle OSiF = 126.8$, $\angle O_1SiO_2 = 98.3$, $\angle SiO_2C = 120.1$, $\angle O_2CO_3 = 177.8$, $\angle O_1SiFO_2 = 102.2$, $\angle SiO_2CO_3 = 180.0$
7	F_2SiO_3C (C_s, **II**)	$R(SiO_1) = 1.536$, $R(SiF) = 1.590$, $R(SiO_2) = 1.939$, $R(O_2C) = 1.214$, $R(CO_3) = 1.142$, $R(CO_1) = 2.272$, $\angle OSiF = 125.1$, $\angle O_1SiO_2 = 92.8$, $\angle SiO_2C = 101.0$, $\angle O_2CO_3 = 163.2$, $\angle O_1SiFO_2 = 100.4$, $\angle SiO_2CO_3 = 180.0$
8	F_2SiO_2C (C_{2v}, **III**)	$R(SiO_2) = 1.672$, $R(SiF) = 1.579$, $R(O_1C) = 1.173$, $R(CO_2) = 1.399$, $\angle OSiF = 116.5$, $\angle O_3SiO_2 = 81.4$, $\angle SiO_2C = 88.0$, $\angle O_2CO_1 = 128.7$
9	$H_6O_4Si_3C{=}O$ (C_{2v}, **IV**)	$R(Si_1O_2) = 1.698$, $R(Si_1O_4) = 1.596$, $R(O_1C) = 1.180$, $R(O_2C) = 1.386$, $R(Si_2O_4) = 1.664$, $R(Si_2H_1) = 1.481$, $R(Si_2H_2) = 1.482$, $\angle O_2SiO_4 = 115.7$, $\angle O_3SiO_2 = 79.5$, $\angle SiO_2C = 88.7$, $\angle O_2CO_1 = 128.4$, $\angle Si_1O_4Si_2 = 164.1$, $\angle O_4Si_2H_1 = 109.4$, $\angle O_4Si_2H_2 = 108.2$, $\angle Si_1O_4Si_2H_1 = 0.0$, $\angle Si_1O_4Si_2H_2 = 120.2$
10	$F_6O_4Si_3C{=}O$ (C_{2v}, **V**)	$R(Si_1O_2) = 1.682$, $R(Si_1O_4) = 1.605$, $R(O_1C) = 1.175$, $R(O_2C) = 1.395$, $R(Si_2O_4) = 1.614$, $R(Si_2F_1) = 1.583$, $R(Si_2F_2) = 1.583$, $\angle O_2SiO_4 = 116.1$, $\angle O_3SiO_2 = 80.7$, $\angle SiO_2C = 88.4$, $\angle O_2CO_1 = 128.7$, $\angle Si_1O_4Si_2 = 171.7$, $\angle O_4Si_2F_1 = 110.3$, $\angle O_4Si_2F_2 = 109.5$, $\angle Si_1O_4Si_2F_1 = 0.0$, $\angle Si_1O_4Si_2F_2 = 120.2$
11	$F_2SiO_2N_2$ (C_s, **VI**)	$R(SiO_1) = 1.516$, $R(SiF) = 1.593$, $R(SiO_2) = 2.145$, $R(O_2N_1) = 1.208$, $R(NN) = 1.114$, $\angle OSiF = 1.114$, $\angle OSiF = 126.7$, $\angle O_1SiO_2 = 99.0$, $\angle SiO_2N_1 = 114.5$, $\angle O_2N_1N_2 = 178.7$, $\angle O_1SiFO_2 = 103.2$, $\angle O_1SiO_2N_1 = 180.0$
12	$F_2SiO_2N_2$ (C_s, **VII**)	$R(SiO_1) = 1.516$, $R(SiF) = 1.595$, $R(SiN_1) = 2.141$, $R(NN) = 1.127$, $R(N_2O_2) = 1.166$, $\angle O_1SiF = 126.5$, $\angle O_1SiN_1 = 100.5$, $\angle SiN_1N_2 = 146.4$, $\angle N_1N_2O_2 = 178.9$, $\angle O_1SiFN_1 = 105.1$, $\angle SiN_1N_2O_2 = 180.0$
13	$F_2SiO_2N_2$ (C_s, **VIII**)	$R(SiO_1) = 1.550$, $R(SiF) = 1.592$, $R(SiO_2) = 1.914$, $R(O_2N_1) = 1.262$, $R(NN) = 1.136$, $\angle OSiF = 123.3$, $\angle O_1SiO_2 = 99.5$, $\angle SiO_2N_1 = 106.7$, $\angle O_2N_1N_2 = 142.4$, $\angle O_1SiFO_2 = 108.1$, $\angle O_1SiO_2N_1 = 0.0$
14	$F_2SiO_2N_2$ (C_{2v}, **IX**)	$R(SiO_1) = 1.666$, $R(SiF) = 1.583$, $R(O_2N_1) = 1.417$, $R(NN) = 1.232$, $\angle OSiF = 114.4$, $\angle O_1SiO_2 = 93.2$, $\angle SiO_1N_1 = 108.6$, $\angle O_1N_1N_2 = 114.8$, $\angle O_1SiFO_2 = 105.6$
15	$F_2SiO_2N_2$ (C_s, **X**)	$R(SiO_1) = 1.663$, $R(SiF) = 1.585$, $R(SiN_1) = 1.774$, $R(O_2O_1) = 1.454$, $R(NN) = 1.212$, $R(O_2N_2) = 1.446$, $\angle O_1SiF = 114.2$, $\angle O_1SiN_1 = 94.5$, $\angle SiO_1O_2 = 107.3$, $\angle O_2N_2N_1 = 115.1$, $\angle O_1O_2N_2 = 111.4$, $\angle N_1N_2Si = 111.8$, $\angle N_1SiFO_1 = 106.8$
16	$F_2SiOC_2H_2$ (C_s, **XI**)	$R(SiO) = 1.519$, $R(SiF) = 1.601$, $R(SiC_1) = 2.484$, $R(SiC_2) = 2.403$, $R(OC_2) = 2.793$, $R(C_2C_1) = 1.207$, $R(C_1H_1) = 1.066$, $R(C_2H_2) = 1.067$, $\angle OSiF = 125.8$, $\angle OSiC_1 = 116.3$, $\angle OSiC_2 = 87.8$, $\angle H_1C_1C_2 = 178.5$, $\angle H_2C_2C_1 = 177.3$, $\angle C_1SiC_2 = 28.5$, $\angle OSiFC_1 = 119.6$, $\angle H_1C_1C_2H_2 = 0.0$
17	$F_2SiOC_2H_2$ (C_s, **XII**)	$R(SiO) = 1.539$, $R(SiF) = 1.604$, $R(SiC_1) = 2.090$, $R(SiC_2) = 2.260$, $R(OC_2) = 2.334$, $R(C_2C_1) = 1.230$, $R(C_1H_1) = 1.071$, $R(C_2H_2) = 1.068$, $\angle OSiF = 123.0$, $\angle OSiC_1 = 105.6$, $\angle OSiC_2 = 73.0$, $\angle H_1C_1C_2 = 155.5$, $\angle H_2C_2C_1 = 176.6$, $\angle C_1SiC_2 = 32.6$, $\angle OSiFC_1 = 114.0$, $\angle H_1C_1C_2H_2 = 0.0$
18	$F_2SiOC_2H_2$ (C_s, **XIII**)	$R(SiO) = 1.703$, $R(SiF) = 1.597$, $R(SiC_1) = 1.819$, $R(SiC_2) = 2.130$, $R(OC_2) = 1.403$, $R(C_2C_1) = 1.344$, $R(C_1H_1) = 1.076$, $R(C_2H_2) = 1.084$, $\angle OSiF = 113.0$, $\angle OSiC_1 = 79.9$, $\angle SiC_1C_2 = 87.8$, $\angle H_1C_1C_2 = 129.9$, $\angle H_2C_2C_1 = 133.4$, $\angle C_1C_2O = 110.9$, $\angle C_2OSi = 86.0$, $\angle OSiFC_1 = 92.1$, $\angle H_1C_1C_2H_2 = 0.0$
19	F_2SiOHC_2H (C_s, **XIV**)	$R(SiO) = 1.624$, $R(SiF) = 1.604$, $R(SiC_1) = 1.798$, $R(OH_1) = 0.960$, $R(C_2C_1) = 1.205$, $R(C_2H_2) = 1.064$, $\angle OSiF = 110.9$, $\angle OSiC_1 = 109.4$, $\angle SiC_1C_2 = 178.4$, $\angle H_2C_2C_1 = 179.7$, $\angle SiOH_1 = 120.7$, $\angle OSiFC_1 = 121.3$, $\angle SiC_1C_2H_2 = 180.0$, $\angle OSiC_1C_2 = 180.0$, $\angle C_1SiOH_1 = 180.0$
20	$F_2SiOC_2H_2$ (C_s, **XV**)	$R(SiO) = 1.549$, $R(SiF) = 1.595$, $R(SiC_1) = 2.062$, $R(OH_1) = 1.546$, $R(C_2C_1) = 1.214$, $R(C_1H_1) = 1.224$, $R(C_2H_2) = 1.067$, $\angle OSiF = 124.0$, $\angle OSiC_1 = 89.5$, $\angle SiOH_1 = 72.9$, $\angle OH_1C_1 = 135.6$, $\angle H_2C_2C_1 = 178.6$, $\angle H_1C_1Si = 62.0$, $\angle H_1C_1C_2 = 157.7$, $\angle OSiFC_1 = 99.3$, $\angle H_1C_1C_2H_2 = 180.0$

* The second column shows the stoichiometric composition of compounds. Their spatial configurations and atom numbering are shown in Fig. 3. Roman numbering (in brackets) corresponds to the numbering of structures in Fig. 3. Bond lengths are in angstroms, and the angels are in degrees. All calculations were carried out using density functional theory at the B3LYP/6-311G** level. The subscripts in the second column correspond to the numbers of atoms in the structures shown in Fig. 3.

Table 4. Total (*E*) and zero-point energies (*ZPE*)*

No.	Structure	Electronic energy, at. u.	*ZPE*, kcal/mol
1	$F_2Si{=}O + O{=}C{=}O$	(–564.61018) + (–188.64114) = –753.25132	5.9 + 7.35 = 13.25
2	F_2SiO_3C (C_s, **I**)	–753.26532	14.1
3	F_2SiO_3C (C_s, **II**)	–753.26155	14.0
4	$F_2SiO_2C{=}O$ (C_{2v}, **III**)	–753.29703	15.4
5	$H_6O_4Si_3C{=}O$ (C_{2v}, **IV**)	–1286.75750	50.0
6	$F_6O_4Si_3C{=}O$ (C_{2v}, **V**)	–1882.78144	30.7
7	$F_2Si{=}O + N_2O$	(–564.61018) + (–184.71328) = –749.32346	5.9 + 7.0 = 12.9
8	$F_2SiO_2N_2$ (C_s, **VI**)	–749.33931	13.8
9	$F_2SiO_2N_2$ (C_s, **VII**)	–749.33778	14.0
10	$F_2SiO_2N_2$ (C_s, **VIII**)	–749.32160	13.5
11	$F_2SiO_2N_2$ (C_{2v}, **IX**)	–749.34962	14.5
12	$F_2SiO_2N_2$ (C_s, **X**)	–749.28480	13.5
13	$F_2Si{=}O + HC{\equiv}CH$	(–564.61018) + (–77.35470) = –641.96488	5.9 + 16.9 = 22.8
14	$F_2SiOC_2H_2$ (C_s, **XI**)	–641.98570	23.9
15	$F_2SiOC_2H_2$ (C_s, **XII**)	–641.98069	23.9
16	$F_2SiOC_2H_2$ (C_s, **XIII**)	–642.05145	26.6
17	F_2SiOHC_2H (C_s, **XIV**)	–642.06543	24.9
18	F_2SiOHC_2H (C_s, **XV**)	–641.95305	21.3

* The second column shows the stoichiometric composition of compounds. Their spatial configurations and atom numbering are shown in Fig. 3. Roman numbering (in brackets) corresponds to the numbering of structures in Fig. 3. Total energies are in atomic units (1 at. u. = 627.5 kcal/mol) and involve total electronic energies and energies of the Coulomb repulsion. Zero-point energies are in kcal/mol. All calculations were carried out using density functional theory at the B3LYP/6-311G** level.

of the intermolecular complex, and its activation energy is 2 ± 2 kcal/mol.

4. Isotopic Exchange $^{16}O \longrightarrow {}^{18}O$ in the $(\equiv Si{-}O)_2Si<^{O}_{O}>C{=}O$ Group

When carbonates are obtained by reactions (I) and (II) at room temperature using molecular oxygen enriched in the ^{18}O isotope (85 ± 2% of ^{18}O and 15 ± 2% of ^{16}O) and $^{12}C^{16}O$ (run A), the C=O group contained a substantial amount of ^{18}O atoms (40 ± 2%) (Fig. 5a, spectrum *1*). Thus, in the product of $C{=}^{16}O$ molecule addition to the dioxysilirane group, the C=O bond contains the oxygen atom from the $>Si<^{O}_{O}$ group with a high probability. Heating the sample at 440 K resulted in further redistribution of IR band intensities at 1931 and 1908 cm^{-1}. The contribution of the second signal to the overall intensity increases from 40 ± 2 to 53 ± 2% (Fig. 5a, spectrum *2*). Thus, the appearance of the ^{18}O atom in the carbonyl group was experimentally observed both in reaction (II) (300 K) and in the thermally activated process of isotopic exchange in the carbonate structure (440 K).

Heating the sample at higher temperatures (>500 K without removal of possible desorption products) and a decrease in the concentration of carbonate groups resulted in the reverse redistribution of the ratio between the intensities of the two bands toward a lower intensity of the signal from the $>C{=}^{18}O$ group. This points to the fact that, at higher temperatures when carbonate decomposition is possible with the elimination of the CO_2 molecule, other reactions also occur in the system. They result in isotopic exchange with the participation of oxygen atoms of the solid surface.

We expected that the thermal decomposition of carbonate (reaction (III)) obtained using ^{18}O-rich oxygen would result in the formation of silanone groups with different isotopic compositions $>Si{=}^{16}O$ and $>Si{=}^{18}O$. However, we failed to register the IR band for the stretching vibrations of a $>Si{=}^{18}O$ bond. According to the literature data, for low-molecular silanones, the isotopic substitution $^{16}O \longrightarrow {}^{18}O$ is accompanied by a long-wave shift of the band corresponding to >Si=O stretching by 35–40 cm^{-1} [1–4]. The band for a silanone group in silica (1306 cm^{-1}) is located on a sharp descent of the band for the fundamental absorbance of the silicon–oxygen skeleton of the matrix. When this band shifts by 35–40 cm^{-1} toward lower wave numbers, it falls into the region, where its registration for the samples used in this work is difficult [9].

The reaction of silanone groups obtained by this method with $^{16}O^{12}C^{16}O$ molecules (run B) at room temperature resulted in the formation of carbonyl groups,

Table 5. Calculated vibrational frequencies of the systems*

No.	Structure	Positions and intensities of IR bands
1	O=C=O	667(33), 667(33), 1376(18), 2436(619)
2	N=N=O	608(8.1), 608(8.1), 1338(56), 2355(344)
3	H–C≡C–H	642(0.0), 642(0.0), 773(96), 773(96), 2069(0.0), 3422(88)
4	$F_2Si=O$ (C_{2v})	321(47), 341(20), 349(90), 810(31), 973(188), 1330(141)
5	$F_2C=O$ (C_{2v})	597(5.4), 619(6.7), 775(38), 964(59), 1228(447), **1991**(468)
6	F_2SiO_3C (C_s, **I**)	47(0.0), 65(1.2), 154(28), 2114(0.5), 220(27), 334(41), 347(0.0), 367(231), 648(35), 651(50), 803(45), 963(186), 1309(160), 1363(30), 2439(772)
7	F_2SiO_3C (C_s, **II**)	–255(62), 82(0.0), 196(1.4), 233(0.2), 270(7.3), 343(34), 354(18), 425(207), 638(32), 649(324), 810(52), 972(189), 1221(65), 1284(176), 2346(625)
8	$F_2SiO_2C=O$ (C_{2v}, **III**)	122(4.5), 208(0.0), 295(15), 295(25), 355(22), 534(2.1), 570(33), 680(17), 774(23), 870(0.6), **901**(223), 1014(205), 1059(283), 1107(405), **1985**(527)
9	$H_6O_4Si_3C=O$ (C_{2v}, **IV**)	24(0.0), 27(0.8), 27(0.2), 29(2.3), 42(0.7), 59(0.0), 124(5.5), 224(0.0), 273(22), 312(18), 332(57), 403(4.3), 525(2.4), 665(0.1), 683(1.4), 712(18), 730(17), 735(0.0), 738(109), 739(158), 793(31), **908**(341), 962(0.0), 964(0.0), 965(148), 966(10), 968(175), 974(1122), 1009(63), 1123(384), 1195(409), 1197(799), **1951**(599), 2256(128), 2257(7.6), 2263(1.5), 2264(234), 2265(0.0), 2266(257)
10	$F_6O_4Si_3C=O$ (C_{2v}, **V**)	9(0.0), 9(0.0), 14(0.0), 15(0.9), 27(1.2), 42(0.0), 104(4.0), 171(0.0), 182(0.0), 222(1.4), 230(1.8), 237(3.1), 272(0.0), 286(11), 302(1.2), 309(0.3), 359(69), 384(0.0), 398(190), 400(105), 411(116), 474(72), 532(4.1), 659(0.5), 682(12.5), 712(12.5), 782(52), 860(110), 891(159), **906**(146), 993(2.5), 1008(0.0), 1008(77), 1011(360), 1013(368), 1109(450), 1208(1247), 1244(629), **1976**(565)
11	$F_2SiO_2N_2$(C_s, **VI**)	52(0.3), 99(1.0), 157(0.2), 169(21), 242(32), 334(43), 349(20), 371(248), 562(7.3), 578(12.5), 802(52), 959(185), 1259(126), 1308(161), 2392(271)
12	$F_2SiO_2N_2$(C_s, **VII**)	37(0.1), 59(1.9), 158(29), 191(1.0), 205(2.5), 333(41), 346(18), 364(247), 604(9.6), 605(7.1), 799(52), 952(181), 1307(154), 1399(41), 2418(588)
13	$F_2SiO_2N_2$(C_s, **VIII**)	–311(73), 92(0.3), 186(0.4), 248(1.6), 338(19), 345(39), 424(11), 449(128), 503(4.2), 596(110), 809(58), 969(186), 1129(46), 1203(282), 2123(190)
14	$F_2SiO_2N_2$(C_{2v}, **IX**)	135(2.1), 189(0.0), 291(13), 293(12), 365(33), 528(30), 599(0.0), 658(48), 740(17), 850(154), 922(32), 983(12), 1001(196), 1025(418), 1535(35)
15	$F_2SiO_2N_2$(C_s, **X**)	115(1.4), 185(0.2), 279(23), 295(1.8), 329(89), 330(28), 508(38), 528(4.0), 641(0.4), 769(40), 835(78), 964(20), 995(195), 1000(271), 1684(160)
16	$F_2SiOC_2H_2$(C_s, **XI**)	77(0.0), 151(2.3), 164(1.4), 187(22), 239(2.7), 327(34), 335(10), 372(230), 659(1.2), 678(0.3), 787(69), 790(77), 808(51), 933(187), 1289(131), 2027(2.4), 3391(186), 3492(6.0)
17	$F_2SiOC_2H_2$ (C_s, **XII**)	–298(26), 136(1.8), 198(2.4), 275(5.7), 340(15), 343(30), 405(0.3), 435(211), 710(37), 713(20), 753(62), 779(4.1), 795(71), 930(188), 1216(146), 1891(67), 3341(149), 3440(31)
18	$F_2SiOC_2H_2$ (C_s, **XIII**)	171(0.8), 215(1.9), 300(15), 327(21), 458(62), 569(23), 664(15), 726(46), 875(66), 934(180), 953(41), 959(160), 1040(151), 1103(99), 1272(8.2), 1547(86), 3196(4.7), 3282(2.7)
19	F_2SiOHC_2H (C_s, **XIV**)	131(0.2), 135(4.4), 178(102), 289(4.6), 315(42), 341(66), 395(52), 402(43), 635(72), 737(31), 741(34), 758(145), 892(315), 941(207), 997(189), 2171(83), 3463(40), 3900(129)
20	F_2SiOHC_2H (C_s, **XV**)	–1004(1124), 90(3.6), 105(16), 174(0.8), 245(4.9), 305(24), 338(22), 439(391), 620(584), 677(15), 794(57), 815(52), 859(30), 959(217), 1225(253), 1653(118), 2149(302), 3437(46)

* The second column shows the stoichiometric composition of compounds. Their spatial configurations are shown in Fig. 3. Roman numbering (in brackets) corresponds to the numbering of structures in Fig. 3. Frequencies are in reciprocal centimeters, and the intensities of IR bands are in km/mol (in brackets). Calculations were carried out using density functional theory at the B3LYP/6-311G** level. The calculated frequencies are not scaled.

which basically have the composition $>^{12}C=^{16}O$ (Fig. 5b, spectrum *1*). However, this band was slightly shifted toward lower wave numbers (1929 ± 1 cm^{-1}). This suggests that the ^{18}O atom is involved in the ring. Heating of the sample for 10 minutes at 430 K resulted in a change in the IR spectrum (Fig. 5b, spectrum *2*). The amplitude of the band for a carbonyl group with a normal isotopic composition decreased and the band of $>^{12}C=^{18}O$ stretching appeared (1897 cm^{-1}). Thus, in this run, thermally activated isotopic exchange with the oxygen atom of a carbonate structure was registered.

Further heating of the sample for 10 min at 520 K resulted in an additional small change in the ratio between the intensities at 1930 and 1897 cm^{-1} (Fig. 5b,

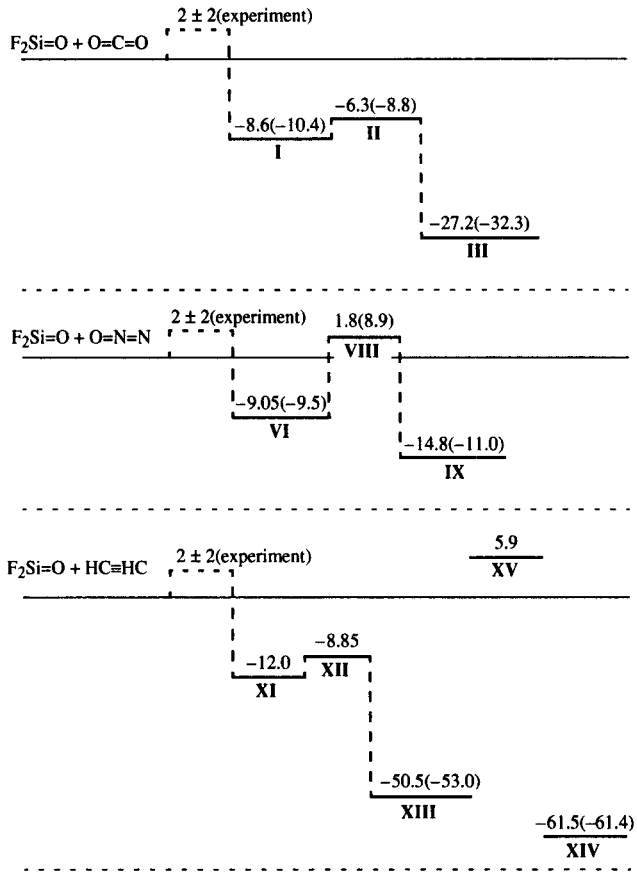

Fig. 4. Energetic diagrams for the systems under study. Numbers are enthalpies of the structures (ΔH_0 at 0 K in kcal/mol) relative to the level of the energies of free molecules (solid line). The first number is the DFT value and the second number is the MP2 value.

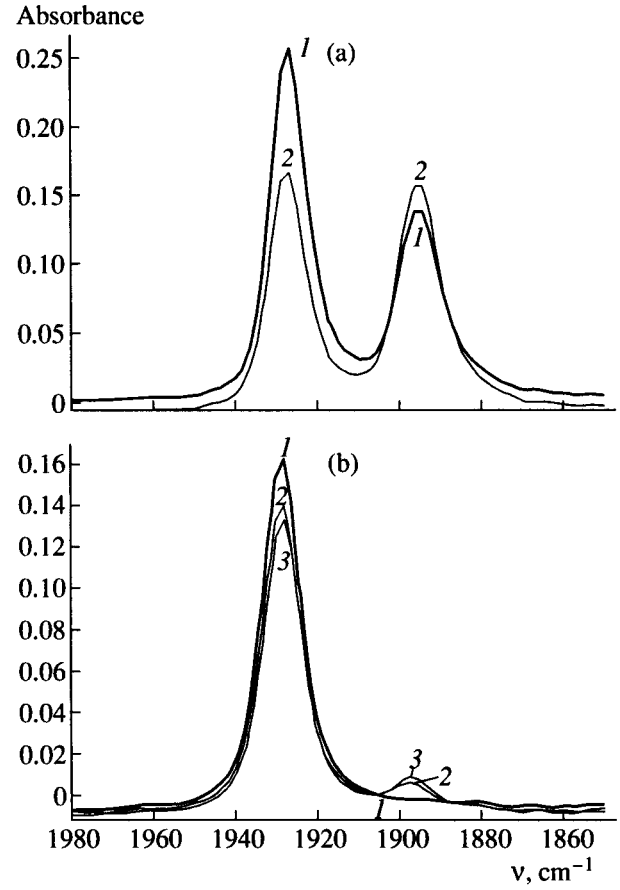

Fig. 5. IR evidence for the isotopic exchange of between oxygen atoms in the carbonate structure: (a) spectrum *1*: carbonates are obtained by reactions (I) and (II) at 298 K using the $^{18}O_2$ molecules (with admixed ^{16}O) and $^{12}C^{16}O$; spectrum *2*: after heating the sample at 440 K for 10 min; (b) spectrum *1*: carbonates are obtained by reaction (IV) $>Si^{18}O(^{16}O) + {}^{12}C^{16}O_2$; spectrum *2*: after heating the sample at 430 K for 10 min; spectrum *3*: after heating the sample at 480 K for 10 min.

spectrum *3*). This may suggest that the ratio between the intensities of these two bands corresponds to the statistical distribution of ^{18}O atoms over three possible positions in the carbonate structure. The corresponding equilibrium is reached at 430 K.

When carbonate is formed by reactions (I)–(II) using the isotope-enriched molecular oxygen and carbon monoxide $^{12}C^{16}O$, the fraction of ^{16}O and ^{18}O atoms involved in the structure of the complex was (43 ± 2) and (57 ± 2)%, respectively. Considering their equiprobable appearance in one of the three positions of the carbonate structure, the fraction of the $>C=^{18}O$ group is 57 ± 2%. In run A, after heating the sample to 440 K, the experimentally observed fraction of the $>C=^{18}O$ group was (53 ± 5)%. These data suggest that the isotopic exchange of oxygen in the carbonate structure is very efficient at 430–440 K.

The reaction of thermally activated isotopic exchange of oxygen in the carbonate structure involves a step where some bonds cleave and some bonds rearrange. A radical mechanism of this process can be discarded because the activation energy for the scission of the weakest C–O bond in the ring is higher than 60 kcal/mol (a thermochemical estimate), and the process cannot occur at 430 K with such a high activation energy. However, the isotopic exchange does occur.

Among molecular pathways for the carbonate transformation, the formation of the intermolecular complex and dissociation (reaction (III)) have the lowest activation energies. Both of them are associated with the elimination of the CO_2 fragment from the carbonate structure. CO_2 can be a separate molecule or a part of a complex. This suggests the following mechanism for isotopic exchange: (1) the elimination of CO_2 from the carbonate structure, (2) CO_2 rotation by 180°, and (3) carbonate regeneration.

The pathway of isotopic exchange associated with the decomposition of the carbonate and CO_2 release to the gas phase is unlikely. The activation energy for the carbonate decomposition and molecular CO_2 formation

is (39 ± 3) kcal/mol (see subsection 1 of this paper). Assuming a preexponential factor of $k_0 = 10^{13}$ s^{-1} for the unimolecular process and taking a minimal value of the activation energy of 36 kcal/mol, we obtain that the rate constant is at most 5×10^{-6} s^{-1} for 430 K. In this case, this process may occur at a noticeable rate at temperatures higher by 100 K than those at which isotopic exchange is observed. Therefore, the isotopic exchange occurs under the conditions when the total energy of the system is lower than the barrier to carbonate dissociation.

The intermolecular silanone–CO_2 complex corresponds to the bound state of the system. We may assume that CO_2 mobility increases in this state. If it will be able to rotate by 180° around the carbon atom, then upon the reduction of the carbonate structure oxygen atoms will exchange places (if oxygen atoms are ^{16}O and ^{18}O isotopes, isotopic exchange will take place). To preserve the system in the bound state, the activation energy of rotation should not be higher than several kilocalories per mole or the process should occur via a tunneling mechanism.

The ^{18}O atom was found in the carbonate carbonyl group in the products of $C={}^{16}O$ addition to the dioxasilirane group at room temperature (see subsection 3). Earlier Radtsig [25] hypothesized carbonate formation in two steps:

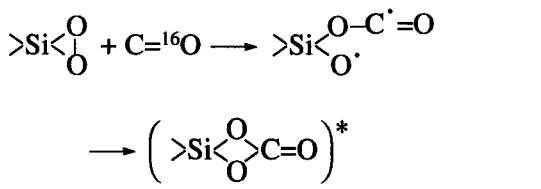

In the first, rate-limiting step, the $>Si(O^{\cdot})(O{-}C^{\cdot}=O)$ biradical is formed, which then recombines to form the carbonate. The product has a substantial amount of excess energy: the reaction heat is ~95 kcal/mol. Most of this energy is evolved in the step of carbonate formation. If the mechanism of isotopic exchange is the same as in the case of the thermally activated process (see above), then it should occur under nonequilibrium conditions when the required energy is available to the system (ring) due to the chemical reaction (chemical activation [26]). For that, isotopic exchange should occur for the lifetime of the "hot ring" on the solid surface (10^{-11}–10^{-12} s).

5. Structure of the Product of N_2O Addition to the Silanone Group

Silanone groups stabilized on the silica surface react with N_2O molecules (k(298 K) ≥ 3×10^{-17} cm^3 molecule^{-1} s^{-1}, $E_{app} = (2 \pm 2)$ kcal/mol). The reaction is accompanied by the disappearance of the IR band of a silanone group at 1306 cm^{-1} and the appearance of the product band at 1448 cm^{-1} [9].

The product formed in the reaction slowly decomposes at room temperature. The process is accompanied by the elimination of the N_2O molecule and silanone group regeneration. The rate constant of this reaction was measured by the optical method from an increase in the intensity of the absorption band of silanone groups at 220 nm [9]: k(295 K) = $(1.5 \pm 0.5) \times 10^{-4}$ s^{-1}. The estimate of activation energy for the decomposition reaction is $E = (23 \pm 1)$ kcal/mol assuming a preexponential factor of 10^{13} s^{-1}. Therefore, the heat of N_2O addition to the $(\equiv Si{-}O)_2Si{=}O$ group is $\Delta H = E - E_{app} = (21 \pm 3)$ kcal/mol.

The structures of possible products in this reaction were analyzed by the methods of quantum chemistry. The calculations were carried out for two four-membered cyclic structures (one of which is an analog of a carbonate group) and two five-membered cyclic structures **IX** and **X**:

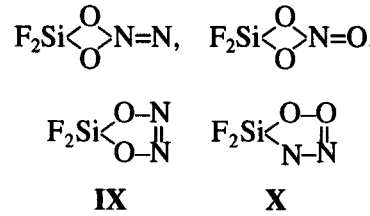

IX **X**

The DFT and MP2 calculations showed that the local minimum on the potential energy surface corresponds only to the **IX** and **X** structures (Fig. 3 and Tables 3–5). The energy of **X** was 23.8 (32.3) kcal/mol higher than the energy of free molecules. Therefore, it can be considered a metastable product. The cyclic azo compound **IX** is a stable product of silanone reaction with N_2O. Table 5 specifies the results of calculations of the vibrational spectrum of **IX**. The stretching vibration of the N=N bond is characterized by the highest vibration frequency, and only this frequency falls in the spectral range where the band of the product (1448 cm^{-1}) was registered. Arrows in Fig. 3 show atomic shifts for this normal vibration. For empirical correction (1) of the calculated frequency of this vibration, we used the F–N=N–F molecule. In this molecule, as well as in **IX**, nitrogen atoms have electronegative substituents (fluorine atoms). For two isomeric forms of this molecule (*cis* and *trans*), the experimental frequencies of N=N stretching are 1525 (cf. calculated 1610) and 1523 (cf. 1637 calculated) cm^{-1}, respectively [22].

After the correction, the value of N=N stretching frequency in **IX** is 1454 cm^{-1} (*trans* isomer) or 1429 cm^{-1} (*cis* isomer). They compare favorably with the experimental data. A decrease in the frequency of N=N stretching when passing from the F–N=N–F molecule to the cyclic structure is due to the internal strain in the cycle, which results in a small elongation of the N=N bond and in a decrease in the force constant. As calculation shows, the position of this band remains almost unchanged when oxygen atoms are substituted by isotopes ($^{16}O \longrightarrow {}^{18}O$). The band shifts by 0.1 cm^{-1}.

Thus, the band at 1448 cm^{-1} suggests that the cyclic azo compound is the main product in the reaction of silanone with N_2O at room temperature.

Quantum chemical calculations show that on the potential energy surface for the $N_2O + F_2Si{=}O$ system, other local minima also exist. Figure 4 shows the energetic diagram for this system. Figure 3 (structures **VI** and **VII**) and Tables 3–5 present information on two intermolecular complexes between the O=N=N molecule and the silanone group. They differ in the orientation of N_2O relatively to the silanone group. In **VI**, the silicon atom is adjacent to oxygen. In **VII**, this atom is adjacent to a nitrogen atom. They have comparable heats of formation: –9.05 (–9.5) and –7.9 (–10.4) kcal/mol. In the IR spectra of both complexes, an intense band for N=N stretching should be observed. The frequency of this stretching in a free N_2O molecule is 2224 cm^{-1} [22] (cf. 2355 cm^{-1} calculated). Upon correction (1), the frequencies of this vibration in **VI** and **VII** are 2259 and 2283 cm^{-1}, respectively. None of these bands was registered in the products of reactions between N_2O with silanone groups at room temperature. Therefore, intermolecular complexes are short-lived intermediates in the process of cyclic azo compound formation.

Figure 3 shows the transition state (structure **VIII**) for the transformation of the intermolecular complex into a cyclic azo compound and the directions of atomic shifts when the system moves along the reaction coordinate. Tables 3–5 specify other characteristics of the transition state.

Note that for the $CO_2 + F_2Si{=}O$ system, DFT and MP2 calculations gave close results, although for the $N_2O + F_2Si{=}O$ system, DFT more accurately describes the experiment. This concerns both the activation energy and enthalpy for the formation of the main product. Therefore, in further discussion, we employ only the results of DFT calculations.

Taking into account that the intermolecular complex participates in the process, the kinetic scheme can be written as follows:

$$(\equiv Si{-}O)_2Si{=}O + N_2O \underset{k_{-1}}{\overset{k_1}{\rightleftharpoons}} (\text{complex})$$

$$\xrightarrow{k_2} (\equiv Si{-}O)_2Si\!<\!\begin{matrix}O{-}N\\ \|\\ O{-}N\end{matrix}$$

The rate-limiting step can be inferred by comparing the activation energies E_2 and E_{-1} for two reactions of molecular complex consumption (see the diagram in Fig. 4). The results of calculation show that they are comparable, but because the energy of the system in the transition state is overestimated in calculations the step of complex formation appears to be rate-limiting.

6. Reaction $(\equiv Si{-}O)_2Si{=}O + HC{\equiv}CH \longrightarrow (\equiv Si{-}O)_2Si\!<\!\begin{matrix}O\\ \diagdown\\ C(2)H\\ \|\\ C(1)H\end{matrix}\!>$

Silanone groups actively react with the molecules of unsaturated hydrocarbons. In the reaction with acetylene at 298 K, one silanone group adds one gaseous molecule [9]. The rate constant of this reaction is $k(298\ K) > 3 \times 10^{-17}$ cm^3 $molecule^{-1}$ s^{-1}. The reaction is accompanied by a change in the sample IR spectrum: the band for silanone groups at 1306 cm^{-1} disappears and two new bands at 3155 and 3081 cm^{-1} appear [9].

We may expect that the reaction of the silanone group with an acetylene molecule occurs via the addition of a C≡C bond or insertion into a C–H bond:

$$(\equiv Si{-}O)_2Si{=}O + HC{\equiv}HC \longrightarrow (\equiv Si{-}O)_2Si\!<\!\begin{matrix}O\\ \diagdown\\ C(2)H,\\ \|\\ C(1)H\end{matrix}\!> \quad (V)$$

$$(\equiv Si{-}O)_2Si{=}O + HC{\equiv}CH \longrightarrow (\equiv Si{-}O_2)Si\!<\!\begin{matrix}O{-}H\\ \diagdown\\ C{\equiv}C{-}H\end{matrix}\!>. \quad (VI)$$

The IR bands appearing in the spectrum are in the region of C–H bond absorption, C being connected to another C via a double bond [27]. This is evidence that the reaction prefers the first channel. Quantum chemical calculations support this conclusion.

Figure 3 shows the structure of the $F_2SiOC_2H_2$ molecule (**XIII**) and Tables 3–5 describe its characteristics. To correct the calculated stretching vibrations of C–H in $F_2SiOC_2H_2$ using formula (1) we used the data on the HFC(2)=C(1)HD molecule [27] in which hydrogen atoms are in *cis*-configuration (ν_{exp}(C(1)–H) = 3095 cm^{-1}, ν_{calc}(C(1)–H) = 3413 cm^{-1}, ν_{exp}(C(2)–H) = 3080 cm^{-1}, and ν_{calc}(C(2)–H) = 3426 cm^{-1}). Upon correcting the calculated values, we find that the frequency of C(1)–H bond stretching in $F_2SiOC_2H_2$ is equal to 3158 cm^{-1}, and this value is 3080 cm^{-1} for the C(2)–H bond, which agrees with the experiment. The C(1)–H bond has a higher frequency of stretches and a lower intensity. A lower frequency for the C(2)–H is explainable by the effect of the electronegative substituent (oxygen).

The formation of rather strong (~10 kcal/mol) intermolecular complexes was characteristic of the systems studied. Figure 3 shows the structure of the complex (**XI**) of $F_2Si{=}O$ and HC≡CH. This structure is typical of a π-complex. A bond is formed between the low-coordinated silicon atom of the silanone group and one of the π-bonds of acetylene.

The intermolecular complexes studied of the silanone with different molecules have close heats of formation (~10 kcal/mol). In the complexes, a portion of electron density (~0.1e) from the CO_2, N_2O, and HC≡CH molecules transfers to the silanone molecule

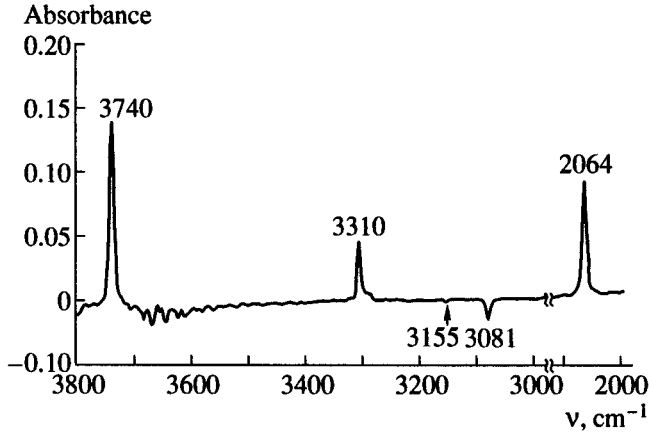

Fig. 6. Differential IR spectrum characterizing the thermal transformation of surface $>Si<^{O}_{CH}>$ CH groups (the initial spectrum is subtracted from the spectrum of the sample heated for 10 min at 750 K).

(these are donors and an acceptor, respectively). This transfer occurs via a low-coordinated silicon atom. However, in the silanone molecule, this charge is distributed between electronegative substituents at a silicon atom (oxygen and fluorine), whereas the charge of the silicon atom remains virtually unchanged.

Figure 3 shows the geometry of the complex–ring transition state (**XII**) for the HC≡CH + F_2Si=O system. The arrows show the shifts of atoms when the system moves along the reaction coordinate.

Figure 4 shows the potential energy surface profile for the HC≡CH + F_2Si=O system for which, as well as for the CO_2 + F_2Si=O system, the complex–ring transition state is below the state of free molecules and the activation barrier is small. Thus, the rate-limiting step of reaction (V) is intermolecular complex formation.

The product of reaction (V) is characterized by relatively high thermal stability: heating the sample to 600 K in a vacuum did not change its concentration (according to IR measurements). Transformations occurred at higher temperatures (750 K). The differential IR spectrum (Fig. 6) shows that the bands at 3155 and 3085 cm^{-1} disappeared from the spectrum upon heating to 750 K, while new intense bands appeared at 3740, 3311, and 2064 cm^{-1}. The band at 3740 cm^{-1} belongs to the region which is characteristic of O–H stretching vibrations in the Si–O–H groups. According to the available literature data [10], the bands at 3311 and 2064 cm^{-1} of comparable intensity should be assigned to C–H and C≡C stretching in the ≡Si–C≡C–H fragment.

The frequency of stretching vibrations of a free hydroxyl group (≡Si–O)$_3$Si–O–H (without a hydrogen bond) on the silica surface is 3749 cm^{-1} [10]. A low-frequency shift (3740 cm^{-1}) of the frequency of ≡Si–O–H group stretching points to a different chemical nature of the coordination sphere of surface silicon atom in the centers formed. For instance, the O–H from the surface fragment (≡Si–O)$_2$Si(H)(OH) has a frequency of 3740 cm^{-1} [29]. However, there is no band for the stretching vibrations of the Si–H bond (2270 cm^{-1}) in our IR spectrum [28]. The simultaneous appearance of the bands at 3740, 3311, and 2064 cm^{-1} suggests that the surface fragment formed in the reaction is (≡Si–O)$_2$Si(C≡CH)(OH). We may assume that a small shift (from 2064 to 2080 cm^{-1} [10]) of the band for C≡C stretching is also due to the difference in the structures of the coordination spheres of silicon in (≡Si–O)$_2$Si(C≡CH)(OH) and (≡Si–O)$_3$Si(C≡CH). This difference has a minor effect on the stretching frequencies of C–H bonds that are distant from the surface silicon atom.

Thermal transformations of the sites did not result in the formation of low-molecular products in amounts comparable to the number of sites. These transformations are intramolecular rearrangements. Alternatively, low-molecular products of pyrolysis adsorb on the silica surface. We cannot rule out that the channel for the transformations considered here is not the only possible one. Unfortunately, it is difficult to obtain the data on the absolute concentrations of registered species using IR spectroscopy.

According to quantum chemical calculation, the F_2Si(C≡CH)(OH) molecule is more stable than its cyclic isomer (see Fig. 4). This agrees with the experimental fact that the cyclic isomer transforms into the linear isomer at higher temperatures when their transformations into each other become kinetically possible. If we know a temperature range where this process takes place, then the activation energy estimate is E_{app} = (52 ± 3) kcal/mol. However, the mechanism remains unclear.

Rearrangement cannot occur via a radical mechanism:

$$(\equiv Si\text{–}O)_2Si<^{O}_{C(1)H}>C(2)H$$

$$\underset{k_{-1}}{\overset{k_1}{\rightleftharpoons}} (\equiv Si\text{–}O)_2Si<^{O^{\cdot}}_{C(1)H}>C(2)H$$

$$\xrightarrow{k_2} (\equiv Si\text{–}O_2)Si<^{O\text{–}H}_{C\equiv C\text{–}H}$$

The rate-limiting step of such a process is the scission of the C–O bond in the ring. Let us estimate the strength of this bond. The heat of reaction $F_2Si<^{O}_{CH}>CH \longrightarrow F_2Si(OH)(C\equiv CH)$ is –10 kcal/mol (Fig. 4) consisting of the endothermic contribution from the C–O scission and the exothermic contribution from the hydrogen atom transfer from the vinyl radical to oxygen. The heat of the second process is 80–85 kcal/mol (the C_β–H bond in the vinyl radical is assumed equivalent to ~40 kcal/mol [29], and the strength of the O–H bond is

120–125 kcal/mol [30]). Therefore, the strength of the C–O bond in the ring is 75–80 kcal/mol. The reaction cannot occur at a noticeable rate with this high activation energy at 750 K.

Let estimate the activation energy of ring opening with acetylene elimination. The calculated heat of the reaction $F_2Si{=}O + HC{\equiv}CH \longrightarrow F_2Si\langle{}^{O}_{CH}\rangle CH$ is –50.5 (–53) kcal/mol. This value is probably somewhat underestimated. The activation energy of acetylene addition to the silanone group is (2 ± 2) kcal/mol. Therefore, we may expect that the activation energy of the reverse reaction (ring decomposition with acetylene elimination) is 55–60 kcal/mol. Taking into account poor accuracy of the above estimates, we may only assume that the corresponding process should occur in the same temperature range as ring transformation.

Because the product of reaction (VI) may be formed via the insertion of the silanone group into the C–H in acetylene, we calculated the activation barrier for a similar process using the ($HC{\equiv}CH + F_2Si{=}O$) system as a model. Figure 3 presents these results. The transition state is **XV** and the arrows show atomic shifts when the systems moves along the reaction coordinate (see Fig. 4 and Tables 3–5). The transition state is higher than the energy of free molecules by 5.9 kcal/mol.[1] The activation energy is probably overestimated in the calculation of the transition state, and the corresponding barrier is lower. Such a mechanism for the formation of the product of reaction (VI) is very attractive. However, more complete kinetic and thermochemical data are needed to prove it.

CONCLUSION

(1) Our experimental IR spectroscopic data and quantum chemical calculations enabled the identification of product structures in the reaction of silanone groups $(\equiv Si{-}O)_2Si{=}O$ with CO_2, N_2O, and $HC{\equiv}CH$.

(2) The data on kinetic and thermochemical characteristics of the processes were obtained. All reactions occur at a high rate at room temperature ($k(298\ K) \geq 3 \times 10^{-17}$ cm^3 molecule^{-1} s^{-1}).

(3) The intramolecular exchange of oxygen was experimentally observed in the $>Si\langle{}^{O}_{O}\rangle C{=}O$ carbonate, and its mechanism was proposed.

(4) Silanone groups form rather strong (~10 kcal/mol) intermolecular complexes with CO_2, N_2O, and $HC{\equiv}CH$ molecules. These complexes are intermediates in the reaction. The data on their structures were obtained.

[1] The activation energy calculated at the same theoretical level for the reaction of H_2 addition to the silanone group is much higher (13.9 kcal/mol), although the C–H bond in acetylene is much stronger than H–H in H_2. The experimental value of the activation energy for the hydrogenation of silanone groups on the silica surface is 13.4 ± 0.3 kcal/mol [11].

ACKNOWLEDGMENTS

This work was supported by the Russian Foundation for Basic Research (grant no. 97-03-32384) and Federal Block Program "Environmentally Clean and Resource-Saving Processes in Chemistry and Chemical Engineering" (The Fundamental Problems of Modern Chemistry Subprogram). Quantum chemical calculations were carried out using Gaussuan'94 [14] at the Zelinskii Institute of Organic Chemistry, Russian Academy of Sciences, within the framework of grant no. 98-07-90290 from the Russian Foundation for Basic Research.

REFERENCES

1. Schnockel, H.J., *J. Mol. Struct.*, 1980, vol. 65, no. 1, p. 115.
2. Withnall, R.W. and Andrews, L., *J. Am. Chem. Soc.*, 1985, vol. 107, no. 8, p. 2567.
3. Arrington, C.A., West, R., and Michl, J., *J. Am. Chem. Soc.*, 1983, vol. 105, no. 19, p. 6176.
4. Khabashesku, V.N., Kerzina, Z.A., Mal'tsev, A.K., and Nefedov, O.M., *Izv. Akad. Nauk SSSR, Ser. Khim.*, 1986, no. 5, p. 1215.
5. Raabe, G. and Michl, J., *Chem. Rev.*, 1985, vol. 85, p. 419.
6. Bobyshev, A.A. and Radtsig, V.A., *Kinet. Katal.*, 1988, vol. 29, no. 3, p. 638.
7. Radtsig, V.A., *Khim. Fiz.*, 1991, vol. 10, no. 9, p. 1262.
8. Radzig, V.A., *Colloids Surf., A*, 1993, vol. 74, p. 91.
9. Radtsig, V.A., Berestetskaya, I.V., and Kostritsa, S.N., *Kinet. Katal.*, 1998, vol. 39, no. 6, p. 940.
10. Morterra, C. and Low, M.J.D., *Ann. N. Y. Acad. Sci.*, 1973, vol. 220, p. 133.
11. Radtsig, V.A. and Senchenya, I.N., *Izv. Akad. Nauk, Ser. Khim.*, 1996, no. 8, p. 1951.
12. Radtsig, V.A., *Kinet. Katal.*, 1996, vol. 37, no. 2, p. 291.
13. Radtsig, V.A., *Khim. Fiz.*, 2000, vol. 19, no. 3, p. 17.
14. Frisch, M.J., Trucks, G.W., Schlegel, H.B., *et al.*, *Gaussian 94, Revision D. 1*, Pittsburgh: Gaussian, 1995.
15. Hehre, W.J., Radom, L., Schleyer, P.V.R., and Pople, J.A., *Ab initio Molecular Orbital Theory*, New York: Wiley, 1986.
16. Becke, A.D., *J. Chem. Phys.*, 1993, vol. 98, no. 7, p. 5648.
17. Lee, C., Yang, W., and Parr, R.G., *Phys. Rev. B: Condens. Matter*, 1988-I, vol. 37, no. 2, p. 785.
18. Scott, A.P. and Radom, L., *J. Phys. Chem.*, 1996, vol. 100, no. 41, p. 16 502.
19. Bobyshev, A.A. and Radtsig, V.A., *Khim. Fiz.*, 1988, vol. 7, no. 7, p. 950.
20. Bobyshev, A.A., Radtsig, V.A., and Senchenya, I.N., *Kinet. Katal.*, 1990, vol. 31, no. 4, p. 931.
21. Radtsig, V.A., Senchenya, I.N., Bobyshev, A.A., and Kazanskii, V.B., *Kinet. Katal.*, 1989, vol. 30, no. 6, p. 1334.

22. Krasnov, K.S. *et al.*, *Molekulyarnye postoyannye neorganicheskikh soedinenii* (Molecular Constants of Inorganic Compounds), Leningrad: Khimiya, 1979.

23. Bunker, B.C., Haaland, D.M., Ward, K.J., *et al.*, *Surf. Sci.*, 1989, vol. 210, p. 406.

24. Morrow, B.A. and Cody, I.A., *J. Phys. Chem.*, 1976, vol. 80, no. 18, p. 1995.

25. Radtsig, V.A., *Kinet. Katal.*, 1996, vol. 37, no. 2, p. 302.

26. Rabinovitch, B.S. and Flowers, M.C., *Quart. Rev.*, 1964, vol. 18, p. 122.

27. Sverdlov, L.M., Kovner, M.A., and Krainov, E.P., *Kolebatel'nye spektry mnogoatomnykh molekul* (Vibrational Spectra of Polyatomic Molecules), Moscow: Nauka, 1971.

28. Radtsig, V.A., Baskir, E.G., and Korolev, V.A., *Kinet. Katal.*, 1995, vol. 36, no. 1, p. 154.

29. Korol'kova, E.M., Radtsig, V.A., and Mel'nikov, M.Ya., *Dokl. Akad. Nauk SSSR*, 1993, vol. 331, no. 2, p. 188.

30. Kazanskii, V.B., Gritskov, A.M., and Andreev, V.M., *Dokl. Akad. Nauk SSSR*, 1977, vol. 235, no. 1, p. 136.